

CRYSTAL DIFFRACTION TELESCOPES FOR NUCLEAR ASTROPHYSICS

P. von Ballmoos, A. Kohnle, J. Naya⁺, J.F. Olive, G.Vedrenne
CESR, 9, av. du Colonel-Roche, 31029 Toulouse, France

R. K. Smither, M. Faiz*, P. B. Fernandez, T. Graber
Advanced Photon Source, ANL, 9700 South Cass Ave., Argonne Ill, USA

ABSTRACT

Until recently, focusing of gamma-radiation was regarded as an impracticable task. Today, gamma-ray lenses have become feasible and present promising perspectives for future instrumentation. For the first time in high energy astronomy the signal/noise ratio will be dramatically improved as gamma-rays are collected on the large area of a lens from where they are focused onto a small detector. Besides an unprecedented sensitivity, such instruments feature very high angular and energy resolution.

Keywords : nuclear astrophysics, gamma-ray spectroscopy, crystal diffraction optics

1. INTRODUCTION

Introductions to high-energy astrophysics traditionally begin by deploring the extreme experimental difficulties this discipline has to deal with. Nuclear astrophysics suffers from a handicap that is ultimately caused by the loss of information during inelastic interaction processes of gamma-ray photons with matter. Unlike the photons at longer wavelengths that mainly undergo coherent scattering in the atmosphere and in the telescopes, gamma-rays interact with matter primarily by incoherent processes. We have become used to accept that it is “impossible to reflect or refract gamma-rays” that have wavelengths two to three orders of magnitude shorter than the distances between atoms in solids.

Consequently, present types of telescopes for nuclear astrophysics make use of inelastic interaction processes : most of the instruments are based on geometrical optics (shadowcasting in modulating aperture systems) or quantum optics (kinetics of Compton scattering). Because the collecting area of such systems is identical to the detector area, nuclear astrophysics has come to a mass-sensitivity impasse where “bigger is not necessarily better”. Improving the sensitivity of an instrument can usually be obtained by a *larger* collection area - in the case of classical gamma-ray telescopes this can only be achieved by a *larger* detector surface. Yet, since the background noise is roughly proportional to the volume of a detector, a larger photon collection area is synonymous with higher instrumental background. The sensitivity is thus increasing at best as the square root of the detector surface.

While space agencies presently express their wish to launch lighter payloads in the future, the new results of SIGMA and GRO indicate that the next generation of instruments should have not only better sensitivities but also better angular and energy resolution.

A possible way out of this impasse consists in reconsidering to take advantage of the phase information of the photons. So far, no telescope relying on elastic coherent scattering has been employed at gamma-ray energies. However, Rayleigh scattering by tightly bound atomic electrons can be significant in high-Z material when very small angles of incidence on a crystal lattice are implied.

⁺ present address : Goddard Space Flight Center, LHEA, Code 661, Greenbelt, MD 20771, USA

^{*} present address : Physics Department, King Fahd University of Petroleum and Minerals, Dhahran 31261, Saudi Arabia

Today, a prototype of a Laue diffraction lens (Fig. 1) has demonstrated its potential in laboratory measurements even at several hundred keV^{1,2,3}: Gamma-rays are focused from a large collecting area onto a small detector volume. As a consequence, the background of the crystal diffraction telescope is extremely low, making possible unprecedented sensitivities.



Fig. 1 The gamma-ray lens and the 3x3 Germanium matrix during the ground based system tests at ANL. When operating in the focal spot of the lens, the Ge detector is located 10-20 m behind the lens.

In this article we present the status and the perspectives of instruments using a crystal diffraction lens in conjunction with a small Ge detector array. The developments and perspectives of collaboration are reviewed in the following sections : the scientific potential of crystal diffraction telescopes is outlined in section 2. In section 3 we summarize the results of a successful test of the ground based telescope system featuring a crystal lens and a germanium detector array. A more detailed description of the principle of crystal diffraction optics is given elsewhere in these proceedings⁴. Section 4 describes the concept of an adjustable lens - a prototype tunable lens is presently undergoing first tests. The project of a crystal lens for use on a balloon gondola is presented in section 5. In section 6 we outline a possible future space borne crystal diffraction telescope using a tunable gamma-ray lens for the energy range relevant for nuclear transitions. We believe that this type of instrument will open new perspectives to observational gamma-ray astronomy.

2. THE SCIENTIFIC POTENTIAL OF CRYSTAL DIFFRACTION TELESCOPES

The characteristics of crystal diffraction telescopes (the fact that one observes in a narrow energy band of typically a few keV with a field-of-view of typically 15-30 arc seconds and with virtually no background) can be exploited for a variety of observational aims: precise source localization, two-dimensional intensity mapping of sources with arc minute extent, the observation of narrow spectral lines, measurement of pulsar light curves in a narrow energy band...

While the first focused cosmic γ -rays may originate from well studied compact continuum sources like the Crab or Cyg X-1, the ultimate potential of a crystal diffraction telescope is in gamma-ray lines. The concept of diffracting a narrow energy band is ideally matched to the narrow lines in the domain of nuclear transitions. A tunable space borne crystal telescope (i.e. the energy that the lens focuses can be changed), would permit the observation of any identified source at any selected line-energy in a range of typically 200 keV to 1300 keV. The fact that the lens is tuned to one energy at a time makes the sites of explosive nucleosynthesis a natural target, where the different decay times and changing opacity to gamma-rays give rise to different gamma-ray lines being dominant at different times after the explosion.

While the evidence for point like sources of narrow gamma-ray line emission has been mostly implicit at this point - besides the supernovae 1987A⁵ and 1991T⁶ - various objects like galactic novae and extragalactic supernovae are predicted to emit detectable gamma-ray lines. These sources should have small angular diameters but very low fluxes - mostly because such objects are relatively rare and therefore are more likely to occur at large distances. The instrumental requirements for exploring this kind of sources match with the anticipated performance of a crystal diffraction telescope:

broad class annihilators: The recent discovery of broad annihilation features in several compact sources ^{7,8,9} has shown that there is one or several types of objects that obviously can produce intense eruptions of positrons. The question is now whether these “broad class annihilators” also generate the positrons that produce the narrow 511 keV line.

The galactic center source 1E1740-29 has been observed by the SIGMA telescope to emit a strong spectral features in the energy interval 300-700 keV that emanated and vanished within days. Radio observations of this object reveal the presence of an AGN like structure with double sided radio jets emanating from a compact and variable core. If the “broad class annihilator” indeed is associated with the radio source, the origin of its high energy emission becomes a key question for gamma-ray astronomy.

Featuring a sensitivity of $\sim 10^{-6}$ ph \cdot cm⁻²s⁻¹ at 511 keV and an angular resolution of 15”, a spaceborne crystal diffraction telescope can test hypotheses on the intensity and site of the narrow 511 keV line. If the radio lobes really track twin jets of positrons out to their annihilation sites in the superposed molecular cloud, a space borne telescope could localize the annihilation regions within less than a day: the predicted flux¹⁰ of 10⁻⁴ ph \cdot cm⁻²s⁻¹ (‘conservative number’) from the outer lobes of the jets would result in 5 σ detections in a few hours.

Novae : The detection of nuclear gamma-radiation from classical novae can offer unique insights into the conditions within the burning regions and the dynamic processes initiated by the runaway explosion¹¹. The high temperatures during the thermonuclear processes induce proton captures on most nuclei in the burning region, transforming stable seed nuclei into unstable proton rich nuclei. The extreme temperature gradient across the envelope at the peak of the burning produces rapid convective energy transport which can mix the envelope material. Large numbers of unstable nuclei with lifetimes longer than the convective time scale could appear at the surface where they are in principle detectable from their nuclear decay or positron annihilation gamma rays (table 1). Unstable nuclei with even longer lifetimes (greater than a few days) could survive the ejection and thinning of the envelope. Then their decay could be observed in gamma rays even if their yields are relatively small.

Since the frequency of Nova explosions in our galaxy is about 40 per year, this kind of object is a very attractive candidate for point source gamma ray line observations. A few hours after the explosion the emitted lines will be blue shifted ($\Delta E \approx 0.7\%$) as the observer would see only the emission from the approaching ejecta ($v \approx 2000$ km/sec) due to the optically thick medium¹². This is relevant for the profile of the 511 keV line that is produced mainly during the first day of the explosion. The evolution in time over the first two hours is dominated by the positron annihilation produced by the ¹³N decay while the ¹⁸F decay dominates later.

line energy	width	mechanism	time scale	mass produced
478 keV	~ 6 keV	${}^7\text{Be}$ (EC) ${}^7\text{Li}$ (10.4 %)	53.3 d	$10^{-8} M_{\odot}$
511-516 keV	~ 3 keV	$\beta+$ decays of ${}^{13}\text{N}$ (862s), ${}^{14}\text{O}$ (102s), ${}^{15}\text{O}$ (176s), ${}^{18}\text{F}$ (158m)	~ 1 day	N/A
1275 keV	16 keV	${}^{22}\text{Na}$ ($\beta+$) ${}^{22}\text{mNe}$ (90.4 %)	3.75 y	$1.6 \cdot 10^{-7} M_{\odot}$

Table 1 : observable gamma-ray lines from novae

After the first few days from the explosion the emitting material will become optically thin to the gamma rays so blue- and red shifted material will contribute to the observed flux, in which case a broadening ($\Delta E \approx 1.3\%$), but not a net shift of the line is expected.

It has been pointed out that novae are possibly significant contributors to the Galactic ${}^7\text{Li}$ abundance - this has important cosmological consequences. The standard model requires that the primordial ${}^7\text{Li}$ abundance must be enhanced by subsequent nuclear nucleosynthesis, while the non-standard models require primordial ${}^7\text{Li}$ to be destroyed by some mechanism in Population II dwarfs. The problem could be clarified if a stellar source of ${}^7\text{Be}$ was identifiable.

supernovae : Deeper insight in the explosive nucleosynthesis using the usual key isotopic decay chains identified for supernovae might be used to constrain the models (at this time, detonation or deflagration) and to understand the dynamics of the explosion through the shape and red (blue) shifts of the gamma-ray lines. The expected fluxes are highly dependent on the models of the different types of SN explosions (especially the convection processes which could remove synthesized materials from the high temperature burning regions). The study of the explosive nucleosynthesis represents a crucial input to better understand the chemical history of the Galaxy.

The nuclear gamma-ray lines from a supernovae that could be observed by a crystal lens are the 847 keV and 1238 keV line from the decay chain ${}^{56}\text{Ni} \rightarrow {}^{56}\text{Co} \rightarrow {}^{56}\text{Fe}$, the 1156 keV line from ${}^{44}\text{Ti}$, and the 1173 keV line from ${}^{60}\text{Fe}$. The photons produced by the nuclei in the shell have noticeable Doppler-shifts due to the motion of the expanding supernova ejecta (a few 10000 km/s). A large broadening of the lines - up to 40 keV at 847 keV is expected for SN type I where the shell gets transparent relatively early. At this energy the bandwidth of a crystal diffraction telescope is about 16 keV FWHM which corresponds to $> 35\%$ of the flux in the SN line. Tuning parts of the lens to different energy bands or scanning the line profile in energy will provide a complete coverage of these potentially broad features.

For supernovae of type II (core collapse SN - the gamma-ray flux is initially obstructed by the massive shell), the broadening is much less accentuated than for SNI's as the observations of SN1987A have shown. A volume of a few Mpc should be accessible to an instrument with a sensitivity of 10^{-7} - 10^{-6} ph $\text{cm}^{-2}\text{s}^{-1}$ ($T_{\text{obs}} 10^6$ seconds) - this will make their detection possible for events occurring within our local cluster.

It has been suggested that the observability of SNIa can be expressed independently of the distance of the host galaxy since the optical peak magnitude of the SN should be directly correlated to the gamma-ray line flux¹³. Indeed, the decay of the ejected gamma-ray isotopes *actually is* the energy source of the optical light curve.

Here, SN1991T has been used to establish a relation between gamma-ray flux f_{847} and optical peak magnitude m_v (the COMPTEL detection of SN1991T⁶ gives $f_{847} \approx (5.3 \pm 2.0) \cdot 10^{-5}$ ph $\text{cm}^{-2}\text{s}^{-1}$ for an optical peak magnitude of $m_v = 11.6$)

$$\log(f_{847}/10^{-4} \text{ ph cm}^{-2}\text{s}^{-1}) = 0.4(10.9 - m_v) \quad (1)$$

According to eq. 1, a detectable flux of $\sim 10^{-6}$ ph $\text{cm}^{-2}\text{s}^{-1}$ is expected from SNIa's with optical peak magnitudes $m_v < 16$. In recent years (2/1987-6/1996), events of this magnitude and brighter were observed at a rate of about three per year¹⁴.

mapping of continuum sources with arc minute extent For sources that have arc minute extent, the narrow field- of view of the lens can be exploited to map the emission intensity. Examples are plerion-type SNRs such

as the Crab Nebula (which will make an excellent scientific objective for a first balloon flight). As the inner regions of the Nebula are governed by the pulsar, the emission intensity distribution within the nebula is determined by the interaction between pulsar and nebula. The nebula size can be understood in the context of magnetohydrodynamic (MHD) bulk-motion models¹⁵. In these models, the energy released by the spin-down of the pulsar is emitted via three components: a relativistic stellar wind of charged particles, a low-frequency, large-amplitude electromagnetic wave, and a toroidal magnetic field originating from the wind-up of the dipole field of the pulsar. The pulsar is at the center of a cavity that is empty except for a relativistic wind and magnetic field emanating from the pulsar. This supersonic wind is expected to terminate at a shock-boundary R_S , where the ram pressure is balanced by the magnetic and particle density of the nebula. Beyond the shock, the particle motions become randomized, leading to intense synchrotron emission. The cavity seen directly around the pulsar in the optical and soft X-ray band places the shock boundary R_S at 10 arc seconds. It has therefore been proposed¹⁶ that the nebula size should not shrink beyond 10 arc seconds with increasing energy.

observation of pulsar light curves Multi-band observations show pulsar light profiles to vary drastically with wavelength. The light curve of the Crab pulsar has been extensively studied by Compton GRO and is seen to vary even within the gamma-ray domain. The low background rate of our telescope can allow the determination of the pulsar light curve profile in a narrow energy band of a few keV. Independent of the pulsar model, the typical pulsar emission energy varies with the position within the magnetosphere, the observation angle with respect to the pulsar magnetic field and the strength of this field. It is thus possible that the pulsar light curve in a narrow energy range is more structured than that obtained in the wide energy band that is typically used for light-curve analysis. If this is the case, the light curves obtained with the crystal lens telescope would be indispensable for the understanding of the geometry of the emission zones within the nebula and the different emission mechanisms. For strong pulsars such as the Crab pulsar (pulsed flux $7.6 \cdot 10^{-5}$ (E/100keV)^{-2.04} ph/cm²s¹keV) or PSR 1509-58, the statistics from one balloon flight will not be sufficient for the determination of a precise light curve, but with a space borne telescope this becomes feasible.

3. LABORATORY PROTOTYPE

A system test of a laboratory crystal diffraction prototype was performed at Argonne National Laboratory³. The experimental setup resembled the classical optical bench consisting in a source, a diffraction lens module, and a detector array.

A characteristic of the ground-based lens is the possibility of focusing a wide range of energies without retuning the lens. To accomplish this, one adjusts the distance from the source to the lens (D_s) and the distance from the lens to the detector (D_d) to match the corresponding Bragg diffraction angle (eq. 2), d is the spacing of atomic parallel planes, θ is the incidence angle measured from the plane, n is an integer, and λ is the wavelength of the incident photon). For small diffraction angles, the relationship between D_s and D_d is the same as for a thin convex lens :

$$2d \sin \theta = n\lambda \quad (2)$$

$$\frac{1}{D_s} + \frac{1}{D_d} = \frac{1}{F}, \quad (3)$$

where F is the focal length of the lens for a given gamma-ray energy. The sources and the geometry used in these experiments are characterized in table 2.

The prototype lens consisted in 416 Ge crystals (1 cm x 1 cm x 1 cm) in six rings. Due to the finite distance between the source and the lens, only a small percentage of the gamma-ray flux incident on the face of an individual crystal will have the correct Bragg angle and be diffracted. However, to optimize the diffraction

efficiency of the crystals, they are divided in three parts by two wedged slots. This partly compensates for the change in the angle of incidence of the photons impinging on the crystals front surface.

A novel gamma-ray detector consisting of a high-purity 3x3 germanium matrix housed in a single cylindrical aluminum cryostat was used for these experiments. Each of the single Ge bars is an n-type coaxial detector with dimensions of 1.5 cm x 1.5 cm x 4 cm and an internal electrode hole of 4-mm diameter. The distance between the front surface and the electrode hole is 1 cm.

Source	Energy [keV]	Activity [mCu]	Focal length [m]	D_S [m]	D_I [m]
^{137}Cs	662	180	10.92	24.75	19.54
^{22}Na	511	50	8.43	19.11	15.09
^{239}Pu	375		6.83	15.47	12.22

Table 2 : Source-Lens-Detector configurations of the system test

The tests have confirmed the feasibility of a telescope system consisting of Ge crystal lens and a Ge detector array. Below we summarize the performance of the ground based prototype

Lens performance The efficiency of the ground based lens can be estimated by :

$$\varepsilon_{diff} = \frac{A_D \cdot N_L \cdot D_S^2 \cdot \varepsilon_{nc}}{n \cdot s \cdot N_D \cdot (D_I + D_S)^2 \cdot \varepsilon_c} \quad (4)$$

where N_L is the count rate of diffracted events by the lens seen by the detector; N_D is the count rate measured by the detector when the lens is removed from the system; D_S is the distance from the lens to the source; D_I is the distance from the lens to the detector; A_D is the area of the detector; n is the number of diffracting crystals in the lens; s is the average surface area of the front side of a single crystal, the detector efficiency used is for a large coaxial Ge detector (6 cm ϕ / 6 cm high) : ε_{nc} is the detector efficiency for a non concentrated beam (31 % at 511 keV); and ε_c is the detector efficiency for a concentrated beam 48 %.

For the 511 keV line, we found $N_L = 153 \text{ c s}^{-1}$ (count rate in the peak, with the lens) - without the lens, $N_D = 77 \text{ c s}^{-1}$ (in the peak). After substitution of the parameters in eq.4, we find that the diffraction efficiency for 511-keV photons is 2.8%, corresponding to an effective diffraction surface of 17 cm².

This low efficiency is due the conditions of operating the lens on the ground : with the Na source being at finite distance; the Bragg relation (eq. 2) is satisfied only for small zones within the wedged crystal. The relatively narrow rocking curve of our present crystals (~2 arc sec) has to be compared to the angular extent of a wedged crystal segment (~30 arc sec). Also, at these distances, a radioactive source is extended (the Na source subtends an angle of ~ 25 arc sec); therefore only a small strip of the source is "seen" by a given zone within a crystal. To some extent, increasing the width of a Ge crystal's rocking curve can improve the lens performance for finite distance / extended sources. Techniques for widening the rocking curve are being studied in collaboration with the Institut Laue Langevin at Grenoble and will be incorporated in future lens prototypes.

At any rate, we would like to stress that the efficiency of the present lens is significantly higher for a source at infinity. For astrophysical point sources, the efficiency is estimated to be ~22% at 511 keV.

Detector performance The segmentation of the 3x3 Ge matrix together with the concentrated beam from the crystal lens allows application of new techniques for background reduction. The method consists of only accepting events that are compatible with the signature of focused photons : i.e. with the focal point of the lens centered on a particular pixel of the array, only photons that deposit any energy in that pixel are considered as "good" events. At 511 keV, the measured percentages of background rejection from an isotropic ambient

background flux are associated with different positions of the focal spot is $\sim 80\%$ for the central pixel. This represents an improvement in the sensitivity by a factor of 2.2 in comparison with a standard detector of the same volume.

Furthermore, the fact that the signal is localized within a small volume of the matrix can be used to define equivalent volumes within other detector pixels that are not receiving signal photons. In this equivalent volume the background count rate can be measured simultaneously to the source observation.

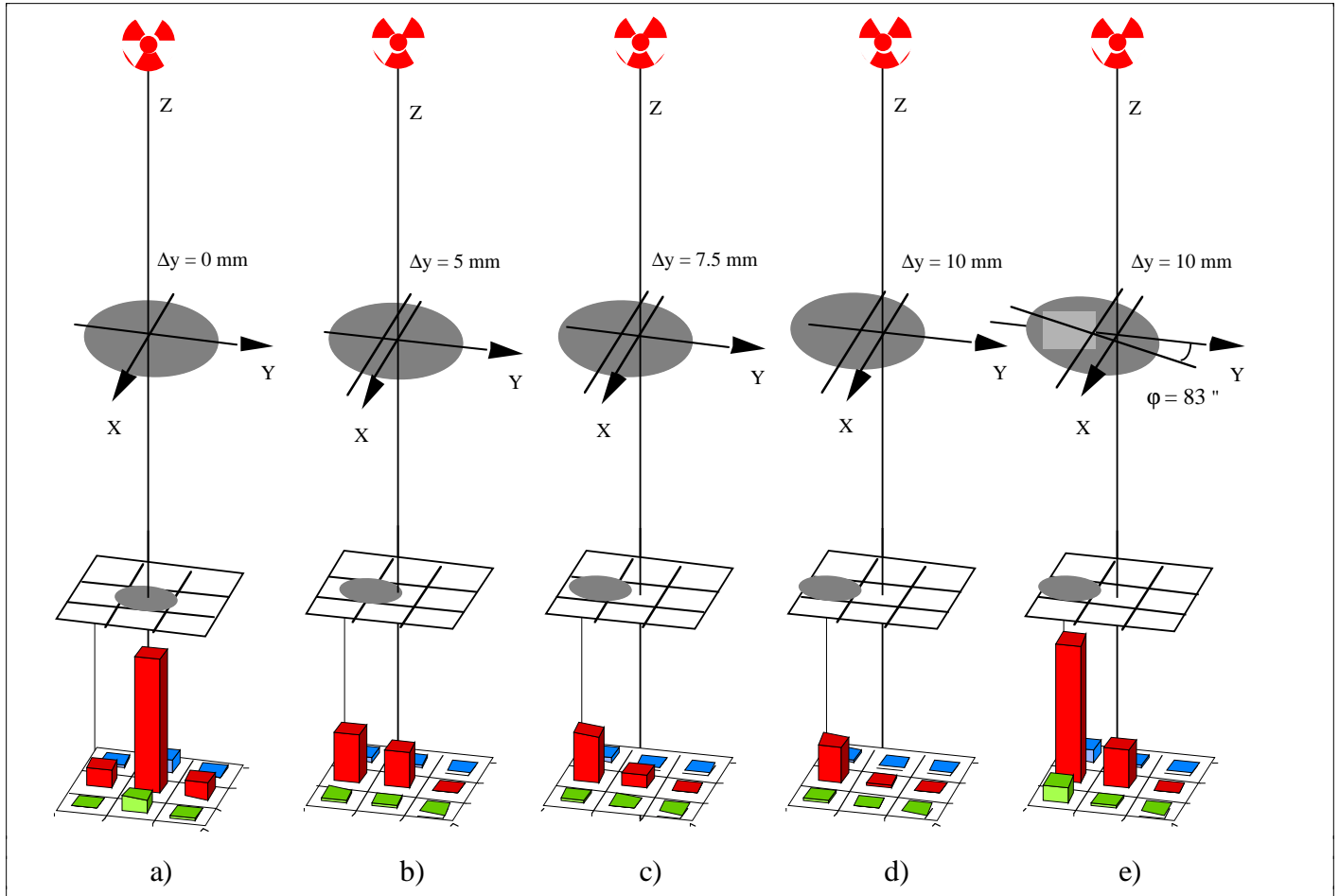


Fig. 2 : Telescope response for focusing off axis sources : a) source, lens, and array are perfectly aligned. b) c) d) evolution of the focal spot position as well as the diffraction efficiency when the lens is displaced along the Y axis. e) lens displaced (10 mm) and tilted ($83''$) such that it is again aligned with the source : the focal spot is on detector 4 and the initial efficiency of the system is recovered.

Off axis source recognition The germanium detector array allows us to take maximum advantage of a focused gamma-ray beam to spatially resolve the source. The focal spot can be localized looking at the 9 count rates. This also allows imaging of an off-axis source. Fig. 2 shows a series of measurements in which the source-lens-detector system has been intentionally misaligned - count rates of the 9 germanium detectors are shown as well as the position of the focal spot with respect to the detector matrix. The gamma-ray energy in this experiment was 662 keV. The movement of the focal spot is evident, as well as the decrease in the intensity of the beam due to the losses of diffraction efficiency because of the misalignment. Finally, the last drawing shows a measurement when the required tilt was applied to the lens in order to match the Bragg condition with a shift of 10 mm. The focal spot is on detector 4, but the initial intensity of the diffracted beam has been recovered.

4. TUNABLE LENS

The Bragg condition (eq.2) indicates that a gamma-ray lens is monochromatic. Since the crystals of the laboratory prototype are adjusted manually, changing the wavelength demands a considerable amount of work. For a space instrument, this limitation would be clearly a handicap. We are therefore developing a tunable gamma lens which permits observation of any identified source at any selected line-energy in a range of typically 200 keV to 1300 keV.

In order to tune the energy band of a crystal lens, two parameters have to be adjusted : the Bragg angle Θ and the focal distance f . While the focal f will have to be known to within \sim a cm, Θ has to be adjusted with a precision of the order of arc seconds.

Figure 3 illustrates the adjustment of the angle Θ . For a lever of \sim 3 cm, the change of the distance z has to occur with a precision better than the rocking curve for a single crystal. i.e. $< 0.25 \mu\text{m}$. Adjusting the lens to an energy $E = E_{\text{ref}} + \Delta E$ requires that each of the single crystal is rocked by an angle $\Delta\Theta$ with respect to the position of a reference energy E_{ref} (i.e. 511 keV) in order to satisfy the Bragg condition anew. Fig.4 shows the precision required for the tuning of the different crystalline planes.

Tuning a crystal (e.g. the [220] planes) from 200 keV to 1300 keV implies a $\Delta\Theta$ of 0.75° corresponding to a displacement of 0.4 mm over a 3 cm lever of the crystal base plate.

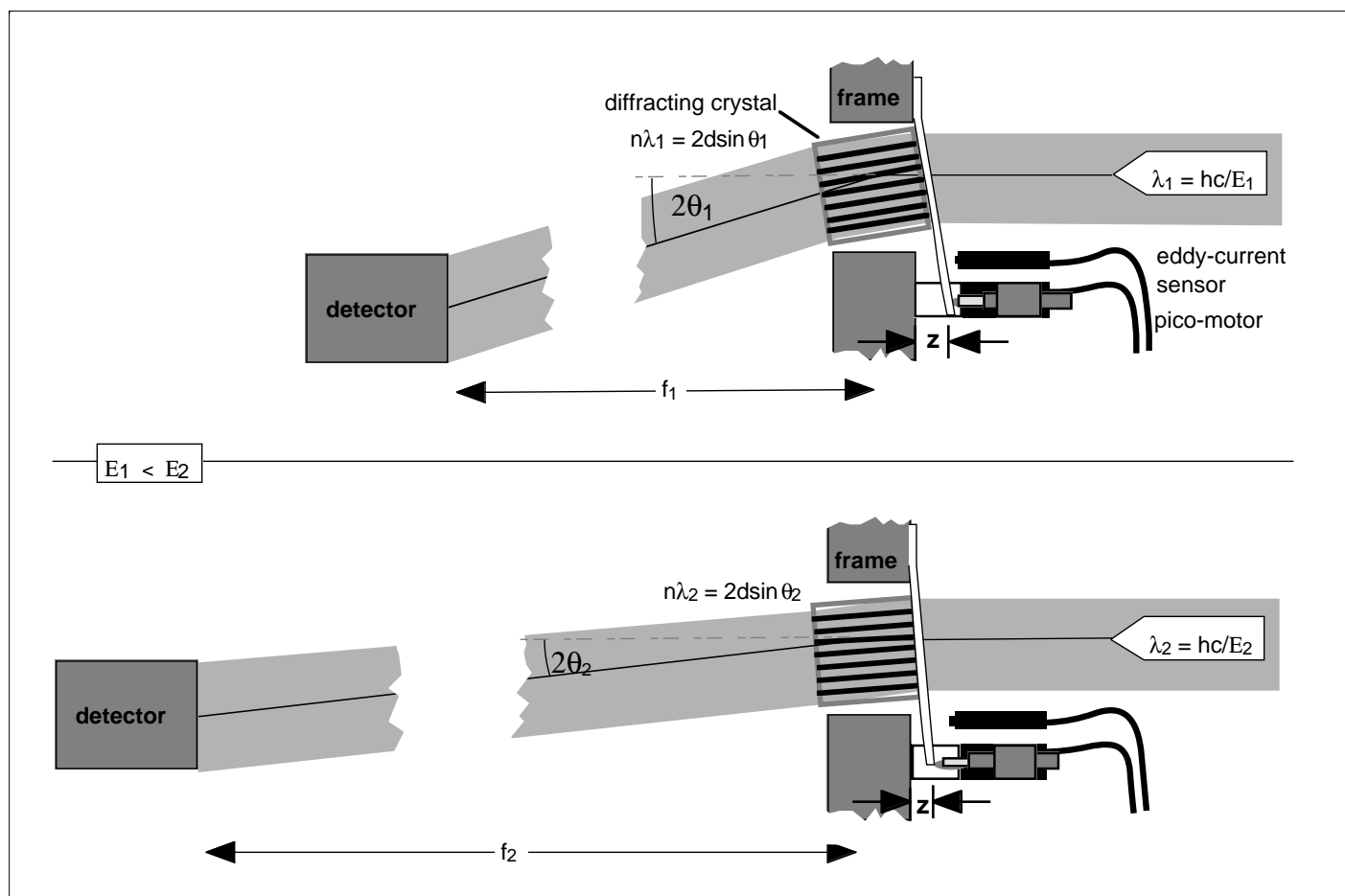


Figure 3 : the principle of lens tuning : in order to tune the energy band of a crystal lens, two parameters have to be adjusted : the Bragg angle Θ and the focal distance f . For a given energy, the diffraction angle θ of a crystal is adjusted by a closed loop system consisting of a piezo-driven actuator that varies the distance z and an eddy-current sensors controlling the displacement.

$$\Delta\Theta = \arcsin(hc/2d(E_{\text{ref}}+\Delta E)) - \arcsin(hc/2dE_{\text{ref}}) \quad (5)$$

$$f = r/2\Theta = \frac{rdE}{nhc} \quad (6)$$

As a first step towards a adaptative gamma lens, we have equipped 28 crystals of the innermost lens ring with miniaturized closed loop drives. Piezo-driven actuators adjust the angle of each crystal while eddy-current sensors measure the displacement. The piezo-motors act on a lever of about 3 cm, the step-size is ~ 15 nm/step, and the maximum drive frequency is 2 kHz. The actuators are controlled via a digital I/O-PC board. Communication with the eddy-current sensors is via RS-232. Individual motors and sensors are addressed by the computer using two external multiplex circuits.

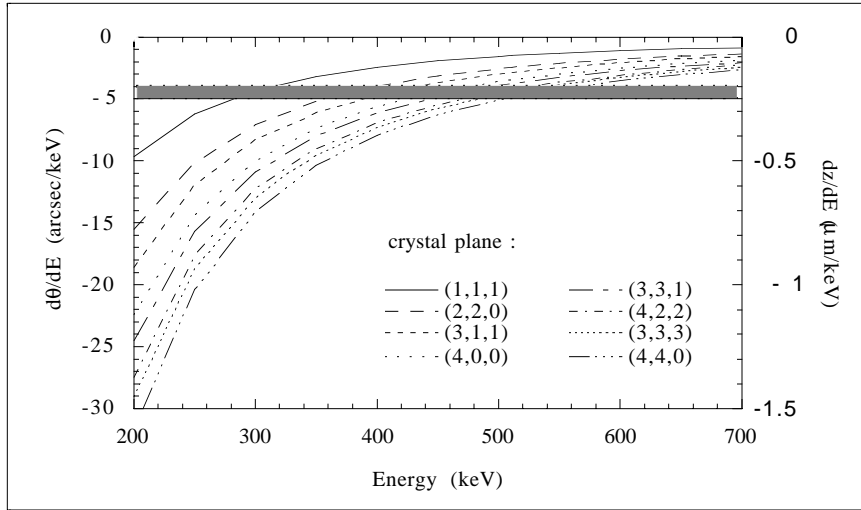


Fig. 4 : required precision for the tuning of the different crystals of the lens. The lever a the baseplates rocking the crystals is 3 cm. For crystals with rocking curves of 10 arcsecs, the precision does not have to be better than ~ 5 arcsec / $0.25 \mu\text{m}$.

5. A BALLOON BORNE GAMMA-RAY LENS

Together with collaborators from the TESRE (Bologna, Italy) and UNH (Durham NH. USA), the teams of the CESR and ANL are proposing a balloon borne crystal diffraction telescope. The development of a monochromatic instrument offers its own outstanding scientific potential as we have shown in section 2. Even during the relative short duration of a balloon flight, a variety of observational aims can be exploited: precise source localization, two-dimensional intensity mapping of sources with arc minute extent, the observation of narrow spectral lines. Furthermore, as a proof of principle, a balloon telescope signifies a compulsory step towards a space borne tunable instrument.

Our collaboration foresees a stepwise development of the balloon borne diffraction lens project : For the first balloon flight, we propose to observe the Crab Nebula with a lens tuned to the energies of 85 and 170 keV having a focal length of 2.7 m and a FWHM field-of-view of 30 arc seconds. This field-of-view will for the first time enable a mapping of the emission intensity at low gamma-ray energies. During this balloon flight, the Crab is expected to be measured with a signal to noise ratios of 3-8. For the first time in this energy range, the detection statistics will be dominated by the source counts - this is a radical novum at gamma-ray energies where signal to noise ratios have traditionally been in the percent range. The choice of a low energy band (meaning small focal length) and a broader field-of-view for the first flight will lessen the demands on gondola pointing and telescope stabilization.

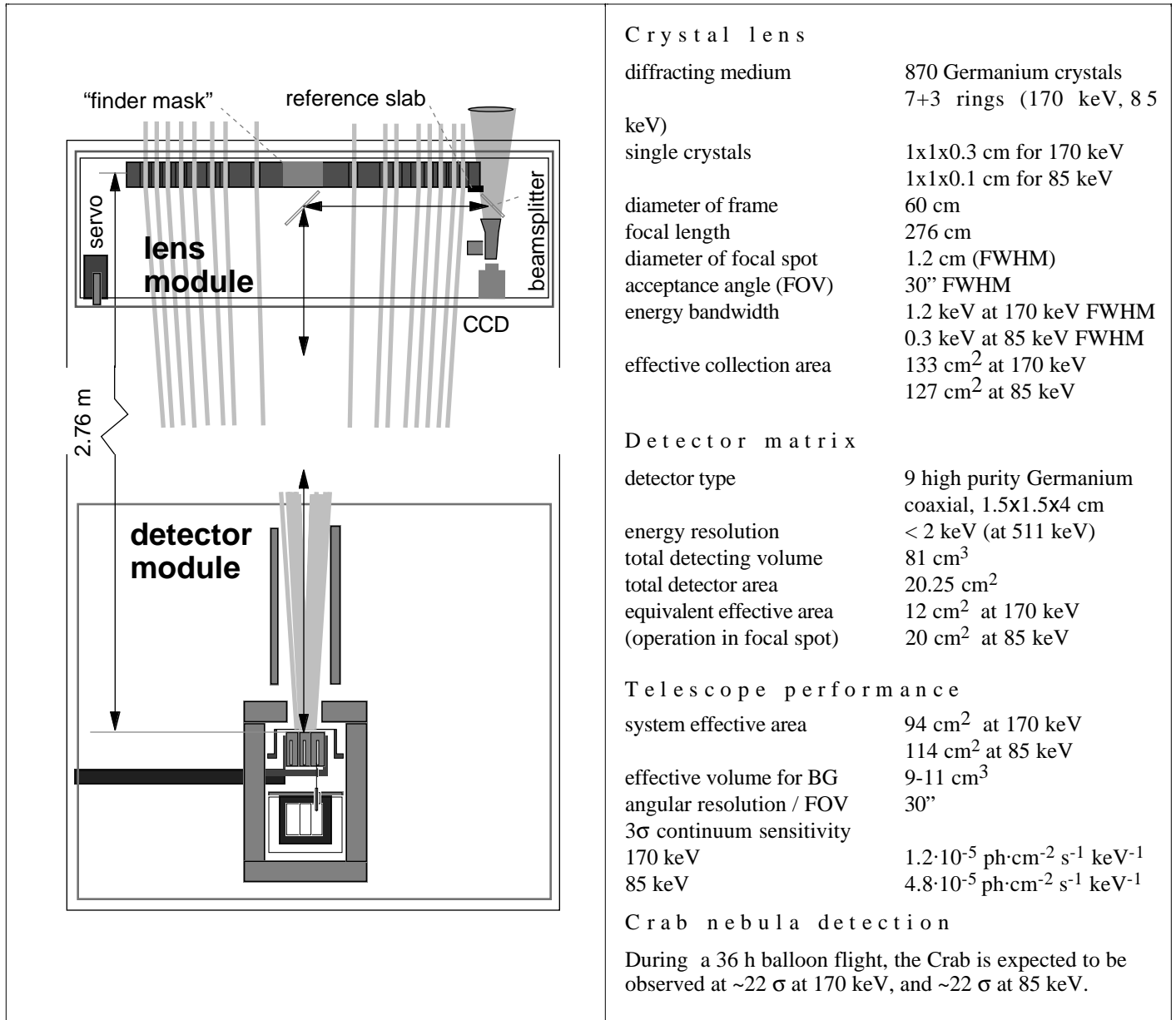


Figure 5 : Layout of the modules within the stabilized structure of the balloon borne crystal diffraction telescope.

Table 3 : Summary of the instrument characteristics and performance of a balloon borne crystal diffraction telescope.

Successive flights will use a lens tuned to higher energies (line energies such as the 511 annihilation line) and have a field-of-view going down to 15 arc seconds. In this configuration (longer focal length, narrower beam) the instrument could help decide whether or not the recently discovered “galactic micro-quasars” are emitting narrow e^+e^- annihilation lines. Other primary scientific objectives may include collapsed objects such as neutron stars, black hole candidates, broad class annihilators, but also novae, supernova remnants, and active galactic nuclei.

The modules within the stabilized telescope structure are schematically shown in Fig. 5, the principal characteristics and the performance of the system are summarized in table 3. At a distance of 276 cm from the detector, the entire lens module is pointed with a precision of about 10 arcmin using conventional stabilization techniques of the gondola (magnetometers). Only the relatively light lens module (~ 20 kg) is pointed with

high accuracy ($\sim 10''$) by a CCD camera that simultaneously views the target area and the lens pointing via an autocollimator cross seen in the alignment mirror. The lens servo drives also compensate for deformations of the structure that occur when the telescope points to different elevations. A beamsplitter and a mirror in the lens module allow to monitor the position of the gamma-ray beam on the detection plane.

The different subsystems of the telescope are designed to be modular in order to allow the progressive implementation and test of more advanced elements : i.e. a diffraction lens that focuses 511 keV photons in the first order, a single Ge detector using pulse shape discrimination (PSD) electronics for radial localization.

A cross-shaped pattern in the central part of the lens frame will be used as a coded mask. Together with the 3×3 Ge matrix, this “finder mask” adds the function of a classical gamma-ray telescope, allowing us to observe sources with a hard X-ray continuum spectrum between 30 keV-200 keV. Besides determining the continuum spectrum of the often variable compact sources, the coded mask mode will verify the main instrument’s efficiency and pointing.

The imaging capabilities of the instrument are defined by its beamwidth which is identical to the field of view of the lens (the field of view depends on the angular width of the mosaic structure of the crystals) : for compact sources discrete pointings of the object will be an appropriate observation mode, while extended structures as for example the jets of galactic microquasars will be scanned with the narrow beam.

6. A TUNABLE CRYSTAL DIFFRACTION TELESCOPE FOR SPACEBORNE OPERATION

Ultimately, the concept of a crystal diffraction telescope should be put to use in space where longer exposures and steady pointing will result in outstanding sensitivities. A space borne crystal diffraction telescope¹⁷ using a gamma-ray lens will consist of a tunable crystal diffraction lens (see section 4) situated on a stabilized spacecraft, focusing gamma-rays onto a small array of germanium detectors perched on an extendible boom (6-19 m). The lens consists of a 90 cm diameter frame accommodating 700 germanium cubes in 11 rings. The 5 inner rings are composed of 1.5 cm thick crystals with an exposed area of 2 cm x 2 cm. Due to their thickness and position on the frame, these rings are optimized for the higher energies. The crystals in the outer 6 rings each have the same geometric area (4 cm²) as the inner ones, yet they are only 0.5 cm thick. These rings are optimized for the lower energies. Above 600 keV they still can be used for diffraction with higher order planes - however with reduced efficiency.

In order to take maximum advantage of the particular properties of a focused gamma ray beam, a germanium matrix will be used similar to the one used during the tests with our ground based telescope (section 2). The matrix consists of 3×5 detector elements, each one with a geometric surface of 3×3 cm and a height of 7-8 cm. The 2.8 cm FWHM focal spot produced by the lens will optimally be pointed at one of the central detector elements. Using isotopically enriched ⁷⁰Ge as detector material will reduce the β^- background component in the energy range of the lens while the enhanced β^+ production only effects the background above 1.5 MeV. Further reduction of the non-localized $n\beta$ components will be possible using the 15 matrix segments. The matrix also offers the possibility to monitor the remaining background simultaneously to the astrophysical observation. Since the spacecraft is seen under a small solid angle, a low intensity of cosmic-ray induced background is anticipated, this will allow us to use a detector shielded only by a very light anticoincidence shield.

Since the focal length of the lens is increasing with energy, a retractable boom (i.e.. a coilable tube mast) will be used to vary the distance between spacecraft and detector along the optical axis of the lens. An energy of 200 keV and 1240 keV respectively corresponds to a change in focal length of 3 m to 20 m - for the 511 keV positron annihilation line the distance lens-detector is 8.3 m. Booms have been used in gamma-ray astronomy on Apollo 15 with a NaI detector and on Mars-Observer for the Ge detectors. In both cases, the extension was around 7 m.

Crystal lens	
diffracting medium	: 700 Ge crystals (2x2x 0.5/1.5cm)
diameter of lens frame	: 90 cm
tuning	: picomotors / eddy current sensors
tunable energy range	: 200 keV - 1300 keV
focal length	: 6.5 m - 19 m
diameter of focal spot	: 2.8 cm FWHM (at all energies)
energy bandwidth	: 6 keV @ 511, 10 keV @ 847 keV
diffraction efficiency	: 25% @ 511 keV, 11% @ 847 keV
effective collection area	: 2800 cm ²
Detector matrix	
detector type	: 15 high purity Ge, coaxial, 3x3x8 cm
energy resolution	: 2 keV (@ 511 keV)
total detecting volume	: 1080 cm ³
total detector area	: 135 cm ²
efficiency at 511 keV	: 54% @ 511 keV, 44% @ 847 keV
Telescope system	
field of view / ang.res.	: 15" FWHM
system effective area	: 370 cm ² @ 511, 275 cm ² @ 847 keV
eff. e volume for BG	: 72 cm ³

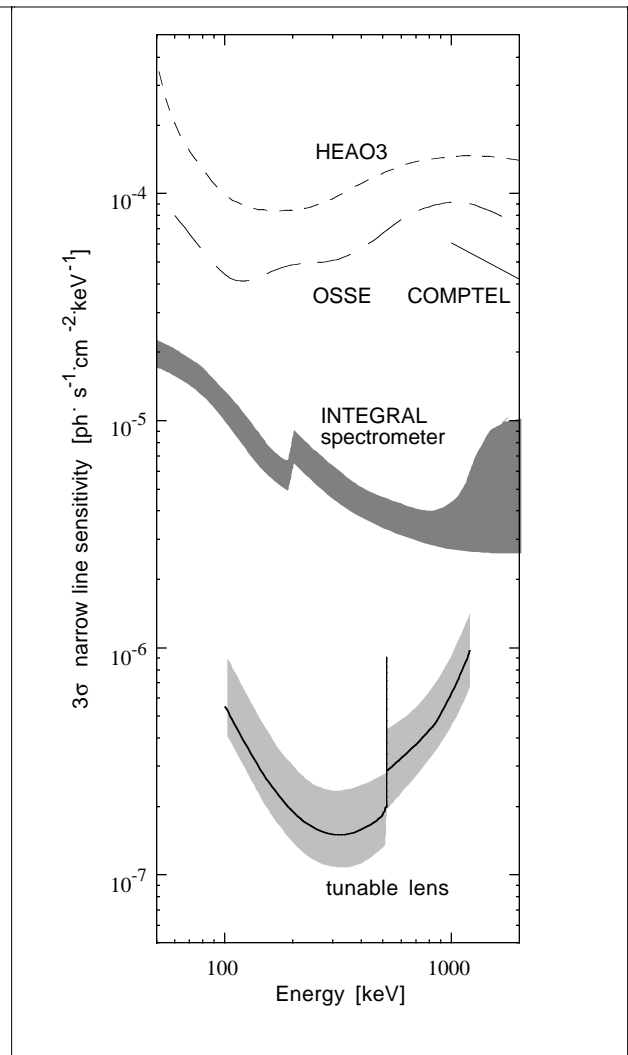


Table 4 : Summary of the instrument characteristics and performance of a tunable crystal diffraction telescope

Figure 6 : estimated sensitivity of a tunable crystal diffraction telescope

Deploying the detector on a boom instead of the diffraction lens has several striking advantages: The mechanical requirements on the mast rigidity are less severe since a Germanium detector array is small and lightweight and thus easy to handle on a boom; moreover, twists and bends of even up to a few cm's are tolerable, as the focal spot (\varnothing 2.8 cm) can wander around on the detector array (total surface 9x15cm) without significant loss of sensitivity. On the other hand, the stringent requirements for the pointing of the lens (typically $\sim 5''$) can be satisfied on board the pointed and stabilized spacecraft. Finally, moving the detector away from the spacecraft reduces the background by up to an order of magnitude. In order to have a mechanically redundant system, the spacecraft will feature two 'detector-boom systems'. If both detectors were to be operated at the same time, different energy-bands could be observed simultaneously, or, maximum sensitivity at one energy band can be achieved by combining the two collector-zones.

The calculations presented here assume a mosaic structure width of $10''$ resulting in a $\Omega \approx 16''$ FWHM for the field of view. For the entire lens the bandwidth is ~ 6 keV at 511 keV, ~ 16 keV at 847 keV. The spectral resolution of present Ge detectors is typically 2 keV at 1 MeV. For a point source at infinite distance we estimate diffraction efficiencies of the order of 26% at 200 keV, 8% at 1000 keV. The full energy peak efficiency of the detector matrix has been calculated by GEANT (80% at 200 keV, 39% at 1000 keV).

We use a background based on the measured ^{70}Ge spectrum of the GRIS detectors during a balloon flight at Alice Springs in 1992¹⁸ - i.e. $2 \cdot 10^{-5} \text{ c} \cdot \text{s}^{-1} \cdot \text{cm}^{-3} \cdot \text{keV}$ at 200 keV, $2 \cdot 10^{-4} \text{ c} \cdot \text{s}^{-1} \cdot \text{cm}^{-3} \cdot \text{keV}$ at 511 keV. Yet, we assume that the ^{70}Ge background can be multiplied by a correction factor $f < 1$ because of lower “shield leakage”- and “ $n\beta^-$ ”- contributions. The intensity of the background is decreasing when a detector is brought away from the “bright” spacecraft (or the earth). This solid angle effect has been demonstrated with a small scintillator that has been deployed on a boom on Apollo 15¹⁹: Compared to the on board spectrum, at a distance of 7 m from the spacecraft, the background in the range 0.2-1.3 MeV was down by a factor of 4-8, at 511 keV even by a factor of 10. For our instrument, we have assumed that the spacecraft induced background will be strongly reduced for the above reason. Furthermore, the resulting low mass (light shield) of the detector module will again reduce the background ($n\beta^-$ and $n\beta^+$ components, see ref.³) as less neutrons are produced compared to the present heavily shielded gamma-ray spectrometers.

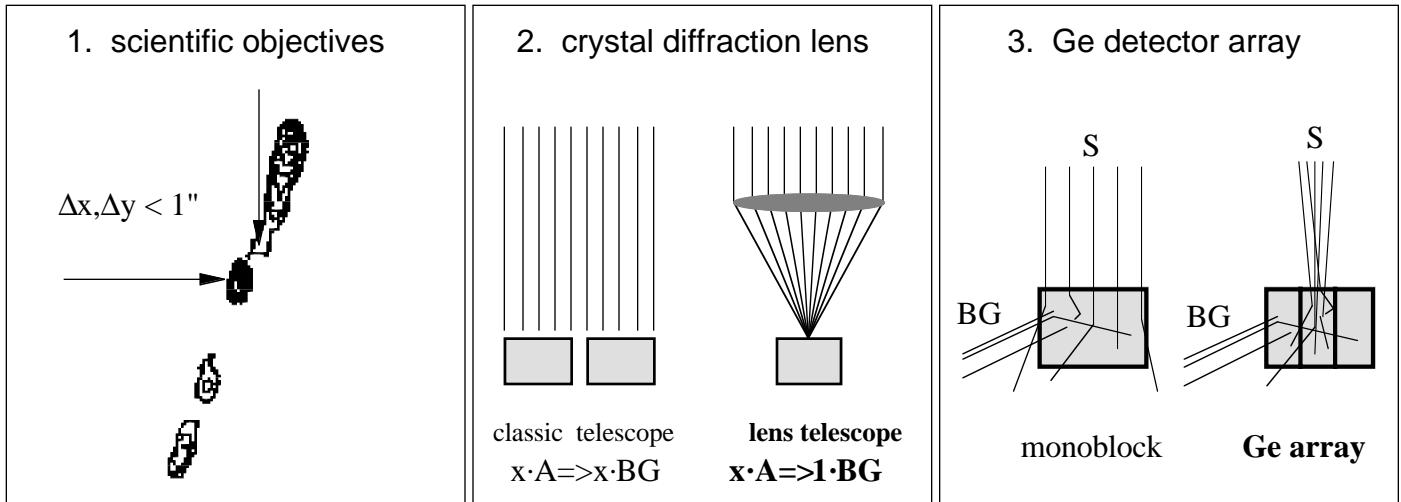


Figure. 7 : The conditions for a focusing gamma-ray telescope : 1) the positions of high-energy sources are known with sufficient precision. 2) a first crystal diffraction lens exists at ANL and has been tested : sensitivity improvements with a large collector and a small detector are practicable. Angular resolution better than a minute and up to a few arc seconds are achievable. 3) Germanium detector arrays allow to take maximum advantage of a focused gamma-ray beam (source localization, further background reduction).

7. CONCLUSION

Even though technically innovative, a crystal diffraction telescope has become feasible today : As summarized in Figure 7, the conditions for operating a focusing gamma-ray telescope are satisfied today: due to the achievements of GRO and SIGMA, scientific objectives at high energies have been identified with position uncertainties less than $1''$; a crystal lens suitable for an astronomical instrument exists and has been tested in the laboratory. The energy-tuning of single crystals is possible using today's piezo-technology; a first tunable lens including 28 closed-loop system is presently being tested; Germanium detector arrays have demonstrated their advantages in conjunction with the prototype lens.

As an R&D project, the tunable gamma-ray lens project is supported by the French Space Agency CNES since 1994. Also, our Laue Crystal Telescope (LCT) is under study as a part of the Hard X-Ray Telescope (HXT)²⁰ which has been selected by NASA for a mission concept study in 1995 (NRA 94-OSS-15, PI HXT : P. Gorenstein, CoI LCT : B. Smither, P. von Ballmoos). A monochromatic lens has been proposed to NASA as an SR&T balloon program (NRA 95-OSS-17) in February 1996.

This work was partially supported by the U.S. DoE Contract No. W-31-109-Eng-38, by the *Region Midi-Pyrénées* (Toulouse) and the French Space Agency (CNES).

REFERENCES

1. Smither R.K. et al, proc. GRO science workshop (Greenbelt, Ma), ed. Johnson et al., 4-539, 1973
2. von Ballmoos P. and Smither R.K. ApJ Sup. S., **92**, 663, 1994
3. Naya et al. , Nucl. Inst. and Meth, A **373**, 159-164, 1996
4. Smither R.K. et al, these proceedings, 1996
5. Matz S.M. et al., Nature **331**, 416, 1988
6. Morris D. et al, proc. 17th Texas Symp. on Rel. Astrophysics, Anals NY Academy of Sciences, Vol **759**, p.397, 1995
7. Bouchet L. et al., ApJ **383**, L45, 1991
8. Goldwurm A. et al., ApJ **389**, L89 1992
9. Briggs M., Ph.D. Thesis, Univ. California, San Diego, 1991
10. Ramaty, R., Leventhal, M., Chan, K.W., & Lingenfelter R., ApJ , **392**, L63, 1992
11. Leising, M. D., Clayton, D. D., ApJ, **323**, 159, 1987
12. Harris, M. J., Leising, M. D., Share, G. H., ApJ, **375**, 216, 1991
13. Arnett W.D., Supernovae : A Survey of current research, p.221, ed M.J Rees and R.J Stoneham (Boston:Reidel), 1982
14. Tsvetkov D.Yu., Pavlyuk N.N., Bartunov O.S., Sternberg Astronomical Institute Supernova Catalogue, <http://www.sai.msu.su/groups/sn/sncat/>, 1996
15. Rees, M.J., and Gunn, J.E. , M.N.R.A.S.,**167**, 1, 1974
16. Aschenbach, B., and Brinkmann, W., A&A, **41**,147, 1975
17. von Ballmoos et al., proc “Imaging in High Energy Astronomy”, Kluwer Dordrecht, p. 239, 1994
18. S.D. Barthelmy, et al. , Ap. J. **427**, 519, 1994
19. Trombka et al., ApJ **181**, 737, 1973
20. P. Gorenstein et al., 187 meeting of the AAS, San Antonio, Texas, Jan 14-18, 1996